Choi, Y., Shin, C, Efficient calculation method of derivative of traveltime using SWEET algorithm for refraction tomography. International Symposium on the Fusion Technology of Geosystem Engineering, Rock Engineering and Geophysical Exploration Seoul, Korea, Nov. 18-19, 2003

Efficient calculation method of derivative of traveltime using SWEET algorithm for refraction tomography

Yunseok Choi, Changsoo Shin
Seoul National University, Seoul, Korea

Abstract: Inversion of traveltime requires an efficient algorithm for computing the traveltime as well as its Frechêt derivative. We compute the traveltime of the head waves using the damped wave solution in the Laplace domain and then present a new algorithm for calculating the Frechêt derivative of the head wave traveltimes by exploiting the numerical structure of the finite element method, the modern sparse matrix technology, and SWEET algorithm developed recently. Then, we use a properly regularized steepest descent method to invert the traveltime of the Marmousi-2 model. Through our numerical tests, we will demonstrate that the refraction tomography with large aperture data can be used to construct the initial velocity model for the prestack depth migration.

1. Introduction

The refraction tomography is being widely used to obtain the velocity structure of the shallow subsurface for the static correction of the reflection data and the engineering site survey. One of the advantages of refraction tomography over reflection tomography is that it can easily pick the first arrival event without human interpretation. However, the refraction tomography has not been widely used for constructing the initial velocity model for the prestack depth migration.

In parameterizing the earth velocity model, tomography can be divided into the block tomography and the cell tomography according to the way in which parameterization is done. Shin et al (1999) introduced refraction tomography by blocky parameterization. They subdivided the velocity model into the blocky layers whose velocity and coordinates of the layers could be changed simultaneously, thereby allowing reduction in the number of unknowns. In the cell-based tomography, we can tessellate the velocity model arbitrarily by small cells or group consisting of several small cells.

In the refraction tomography, we update the velocity model by minimizing the difference of picked traveltime and modeled traveltime of initial model. Refraction traveltime is the first traveltime for a wave emanating from a source to pass through the medium and to arrive at the receiver. Hence, we can express, both explicitly and implicitly, the traveltime as a function of the subsurface velocities, and then calculate the Frechêt derivative analytically.

In this paper, we develop a new algorithm to calculate Frechêt derivative of the traveltime by exploiting SWEET (Suppressed Wave Equation Estimation of Traveltime) algorithm (Shin et al., 2002). We then applied it to the refraction tomography. We will begin by reviewing the SWEET algorithm suggested by Shin et al (2002). Next, we will develop a new algorithm to compute the Frechêt derivative of the traveltime with respect to the subsurface velocity by a numerical structure of the finite element method, a modern sparse matrix technology, and the SWEET algorithm.

By inverting the Marmousi-2 model (Martin et al., 2002) via our algorithm, we will demonstrate that the refraction tomography combined with the long offset survey can provide a smooth velocity model for the prestack depth migration.

2. Theory

Calculation of traveltime and its Frechêt derivative

Scalar wave equation in the time domain is given as

$$\frac{1}{v^2}\frac{\partial u^2}{\partial t^2}-\frac{\partial u^2}{\partial x^2}-\frac{\partial u^2}{\partial z^2}=f \tag{1}$$

where x, z are the coordinates in the horizontal and vertical directions, respectively, v is a velocity function of x and z, t is time, f is a source function, and u is a pressure wavefield or a displacement. In general, the time domain wavefield (u) can be approximated as a series of spikes. (Shin et al., 2002)

$$u(t) = \sum_n A_n \delta(t - t_n) \quad n = 1, \cdots\cdots, \infty \tag{2}$$

where A_n is the amplitude at n th-digitized time (t_n). By multiplying equation (2) by a strong damping factor e^{-st}, we can approximate the damped wavefield as

$$u(t)^* = u(t)e^{-st} \cong A_1 e^{-st}\delta(t - t_1). \tag{3}$$

Integrating equation (3) from 0 to infinity with respect to t results in approximating Laplace transform of equation (2).

$$\tilde{u} = \int_0^\infty u(t)e^{-st}dt \tag{4}$$

where s is the Laplace frequency. Therefore, the Laplace-transformed wavefield at a relatively high and optimum Laplace frequency s (Shin et al., 2002) can be given as

$$\tilde{u} = \sum_n A_n(x,z)e^{-st_n(x,z)} \cong A_1(x,z)e^{-st_1(x,z)}. \tag{5}$$

By taking the derivative of equation (5) with respect to s and dividing it by $\tilde{u}$, we can obtain the traveltime of the first arrival event (Shin el al., 2002),

$$\frac{\partial \tilde{u}}{\partial s} = -t_1 A_1 e^{-st_1} = -t_1\tilde{u}, \qquad \frac{\partial \tilde{u}}{\partial s} = -t_1 A_1 e^{-st_1} = -t_1\tilde{u}. \tag{6}$$

Following Shin et al (2001)'s notation, we parameterize the subsurface by an $N = N_x \times N_z$ elements where N_x is the number of elements in x direction and N_z is the number of elements in z direction. At each element, we identify a velocity v_i. In this manner, we define our model parameter vector $\mathbf{P}$ to be

$$\mathbf{p} = [v_1, v_2, \cdots\cdots, v_N]. \tag{7}$$

Then, the first arrival traveltime can be expressed as a function of a subsurface parameter, thereby allowing us to take derivative of equation of the traveltime with respect to p_i via a simple algebra. Thus the derivative of the traveltime ($\partial t_1 / \partial p_i$) with respect to p_i can be given as

$$\frac{\partial t_1}{\partial p_i} = \frac{\left(-t_1 \dfrac{\partial \tilde{u}}{\partial p_i} - \dfrac{\partial^2 \tilde{u}}{\partial s \partial p_i}\right)}{\tilde{u}} \qquad i = 1, \cdots\cdots, N. \tag{8}$$

From equation (8), we note that the derivative of the Laplace-transformed wavefield with respect to the subsurface parameter (p_i) and the second order derivative of the Laplace-transformed wavefield appear in equation (8). Next we explain how to compute these derivatives via the finite element modeling technique. The finite element or finite difference discretized wave equation in the Laplace domain can be given (Shin et al., 2002) as

$$\mathbf{S}\tilde{\mathbf{u}} = \tilde{\mathbf{f}} \tag{9}$$

where,

$$\mathbf{S} = \mathbf{M}s^2 + \mathbf{K} \tag{10}$$

$$\tilde{\mathbf{u}} = \int_0^\infty \mathbf{u}(t)e^{-st}dt \tag{11}$$

$$\tilde{\mathbf{f}} = \int_0^\infty \mathbf{f}(t)e^{-st}dt \tag{12}$$

where $\mathbf{M}$ is the global mass matrix, $\mathbf{K}$ is the global stiffness matrix, $\mathbf{u}$ is the wavefield vector, $\mathbf{f}$ is the source vector, and s is the Laplace frequency.

If we take the derivative of equation (9) with respect to Laplace frequency s, we will obtain the derivative of the wavefield with respect to s through a simple matrix algebra (Note that $\tilde{\mathbf{f}}$ is constant; we assume that the source function in time is a delta function)

$$(\mathbf{M}s^2 + \mathbf{K})\frac{\partial \tilde{\mathbf{u}}}{\partial s} = -2s\mathbf{M}\tilde{\mathbf{u}}. \tag{13}$$

Of course, we can take the derivative of equation (9) with respect to the velocity parameter p_i, as Shin (1988) did in his waveform inversion, we can express it as

$$(\mathbf{M}s^2 + \mathbf{K})\frac{\partial \tilde{\mathbf{u}}}{\partial p_i} = -s^2\frac{\partial \mathbf{M}}{\partial p_i}\tilde{\mathbf{u}} \quad i = 1, \cdots\cdots, N. \tag{14}$$

For the second derivative of the wavefield, similarly, we take the derivative of equation (14) with respect to s once more and express it as

$$(\mathbf{M}s^2 + \mathbf{K})\frac{\partial^2 \tilde{\mathbf{u}}}{\partial s \partial p_i} = -2s\mathbf{M}\frac{\partial \tilde{\mathbf{u}}}{\partial p_i} - 2s\frac{\partial \mathbf{M}}{\partial p_i}\tilde{\mathbf{u}} - s^2\frac{\partial \mathbf{M}}{\partial p_i}\frac{\partial \tilde{\mathbf{u}}}{\partial s} \quad i = 1, \cdots\cdots, N. \tag{15}$$

In the frequency or the Laplace domain modeling, we, in principle, need to invert the huge sparse matrix arising from the finite element or the finite difference method. However, this is practically intractable and almost impossible for a large scale 2-D or 3-D problems. Thus, instead of inverting the huge sparse impedance matrix, we factor a real impedance matrix into the upper and the lower triangle matrix and then obtain the wavefield by forward and backward substitution (Kreyszig, 1993; Pratt, 1999). In computing $\frac{\partial \tilde{\mathbf{u}}}{\partial s}, \frac{\partial \tilde{\mathbf{u}}}{\partial p_i}$ and $\frac{\partial^2 \tilde{\mathbf{u}}}{\partial s \partial p_i}$, once we factor the real impedance matrix, the computation of these derivatives only require multiple sparse right hand side vectors.

Inversion theory (The steepest descent method)

In travel time tomography, we usually take the residual error between the data and the modeled data, and express it as

$$\delta d_{i,j} = u_{i,j} - d_{i,j} \quad \begin{matrix} i = 1, \cdots\cdots, n_r \\ j = 1, \cdots\cdots, n_s \end{matrix} \tag{16}$$

where $d_{i,j}$ is the modeled data, $u_{i,j}$ is the measured data and i is the number of receiver on the surface and j is the number of shot on the surface. As it is common in geophysical inverse problems, we try to minimize the $l_2 - norm$ of the residual error and express it as

$$\mathbf{E}(\mathbf{p}) = \frac{1}{2}\delta \mathbf{d}' \delta \mathbf{d}. \tag{17}$$

In a classical steepest descent method, we update the velocity model in a steepest descent direction that is perpendicular to the objective function (Lines and Treitel, 1984) by a general iterative rule and modify a classical steepest descent method as (Shin et al., 2001)

$$\mathbf{p}^{(k+1)} = \mathbf{p}^{(k)} - \left[diag\left[\mathbf{J}^t\mathbf{J}\right]\right]^{-1} \nabla_p E^{(k)} \tag{18}$$

where k is the number of iteration, and t denotes the transpose, $\mathbf{J}$ is the $(n_r \times n_s)\times n$ Jacobian matrix, $diag$ means the diagonal elements of the approximate Hessian matrix, n_r is the number of receivers, n_s is the number of shots, and n is the number of parameters. By explicitly computing the Frechêt derivative, we can not only compute $\nabla_p E_j^{(k)}$ by multiplying the residual by the Jacobian matrix but also compute the approximate Hessian matrix. Thus we can express the steepest descent direction as

$$\nabla_p E_j^{(k)} = \frac{\partial E}{\partial \mathbf{p}} = \mathbf{J}^t \delta d \tag{19}$$

where $\mathbf{P}$ is the model parameter vector.

In this paper, we used only the diagonal matrix of the approximate Hessian and added a damping factor to regularize the step length.

$$\mathbf{p}_j^{(k+1)} = \mathbf{p}_j^{(k)} - \left[diag\left[\mathbf{J}^t\mathbf{J}\right] + \lambda \mathbf{I}\right]^{-1} \nabla_p E_j^{(k)} \tag{20}$$

where $\mathbf{I}$ is an identity matrix, and λ is a Lagrange multiplier.

3. Synthetic data examples

Comparison of analytic Frechêt derivative and numerical Frechêt derivative

In classical optimization technique requiring Frechêt derivative, the verification of the exact Frechêt derivative is a crucial element to be checked. Hence we compare analytic Frechêt derivative with numerical Frechêt derivative using finite difference formula (Lines and Treitel, 1984). Figure 1 shows the velocity model chosen for comparing our Frechêt derivatives. This model has five horizontal layers. The horizontal distance is 5km and the vertical distance is 0.5km. We placed the source at 500m on the surface, and receivers are located on the surface at an interval of 10m. For comparison of Frechêt derivative, we perturbed the block denoted by rectangle symbol, as shown in Figure 1.

Figure 2 shows the Frechêt derivative of the traveltime. From Figure 2, we note that both the analytic Frechêt derivative and the numerical Frechêt derivative are in good agreement with each other.

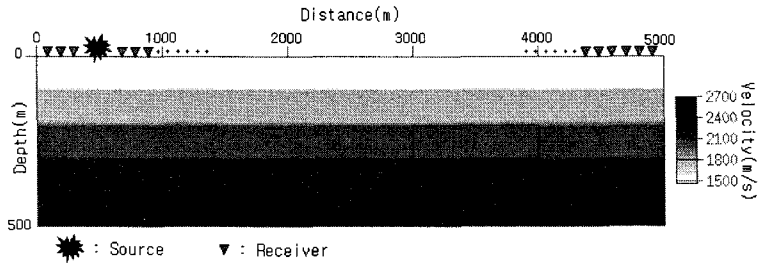

Fig. 1. Five layered model for the comparison of Frechêt derivative by the analytic method with the numerical difference method.

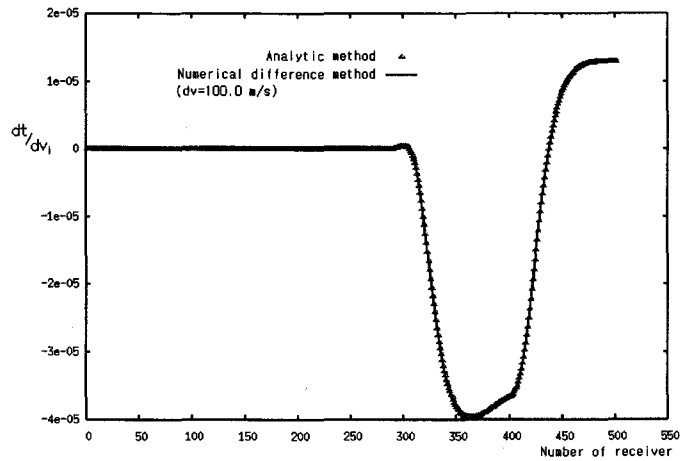

Fig. 2. The analytical Frechêt derivative (dt / dv) of the traveltime where the rectangular block in Figure 1 is perturbed.

Marmousi-2 model (traveltime inversion)

For the traveltime inversion of a large-scale model, we choose a Marmousi-2 model (Martin et al., 2002) that is larger than the original Marmousi model. The main reason for taking the Marmousi-2 model is to increase the illumination zone so that the refracted waves could penetrate deep into the model. Figure 3 shows the Marmousi-2 model whose horizontal and vertical distance are 17km and 3km, respectively. The grid size is 40m. One hundred and five shots are located on the surface at 160m interval while four hundred and twenty six receivers for each shot are placed on the surface at 40m interval. We parameterized the velocity model in two different ways. The first one is parameterizing a velocity model of each cell, while the other is choosing the block which consists of 5×5 cells as unknowns. Figure 4 (a) shows the initial velocity model whose velocity linearly increases with depth, whereas Figure 4 (b) shows the inverted velocity model at the 20^{th} iteration through the cell parameterization. As is common in refraction tomography, we could not recover the true velocity model exactly but was able to obtain the velocity model that vaguely converge the true model. Figure 4 (c) shows the inverted velocity model at the 15^{th} iteration through the block parameterization, which is more vaguely resolved than that of the cell parameterization. Besides that the whole structure appears to be similar to the inverted model of the cell parameterization. Of course, the block parameterization is capable of reducing computation time to 96% reduction of that of the cell parameterization.

Figure 5 shows the history of the $l_2 - norm$ of residual error as a function of iteration. From this figure, we note that $l_2 - norm$ of residual error reach 1~2% of the initial value.

Having successfully inverted the Marmousi-2 model, we proceeded to the Kirchhoff prestack depth migration using the inverted velocity model as an initial model for the Kirchhoff prestack depth migration. Figure 6 (a) shows the depth image based on the initial model, while Figure 6 (b) shows the depth image obtained from the inverted velocity model by the cell parameterization. Lastly, Figure 6 (c) shows the depth image derived from the inverted velocity model by the block parameterization.

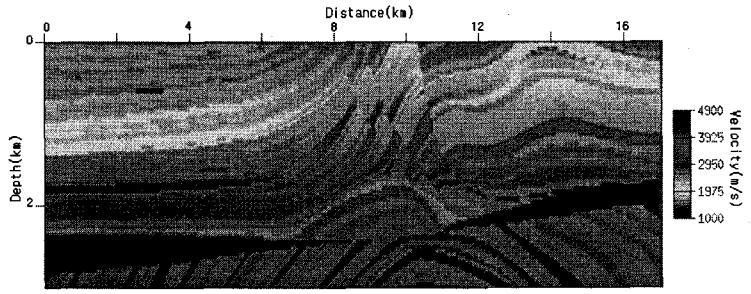

Fig. 3. Marmousi-2 model. The grid interval is 40m.

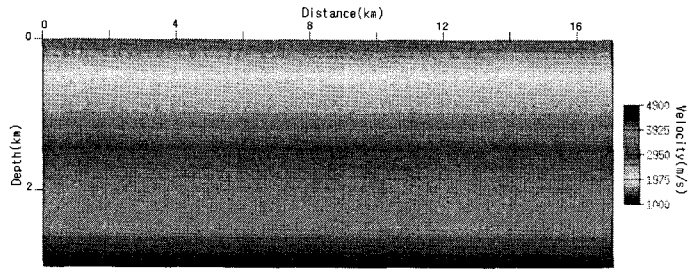

(a)

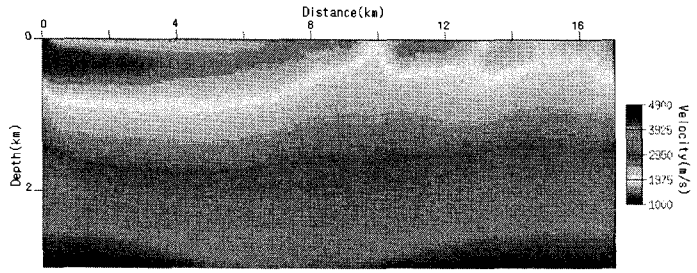

(b)

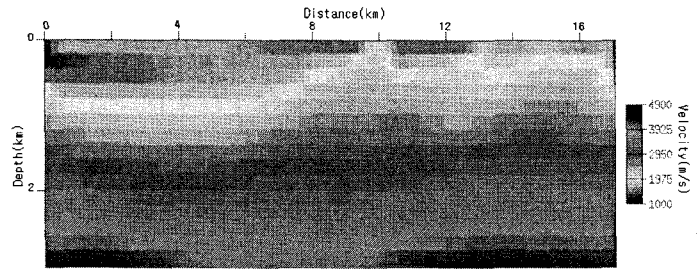

(c)

Fig. 4. The initial model and the inverted model for the inversion of traveltimes of Marmousi-2 model. (a) The initial model whose velocity linearly increases with depth, (b) The inverted model at 20th iteration by the cell parameterization, (c) The inverted model at 15th iteration by block parameterization.

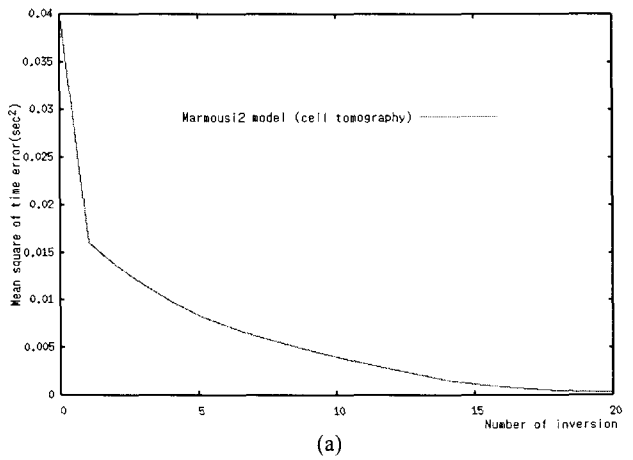

(a)

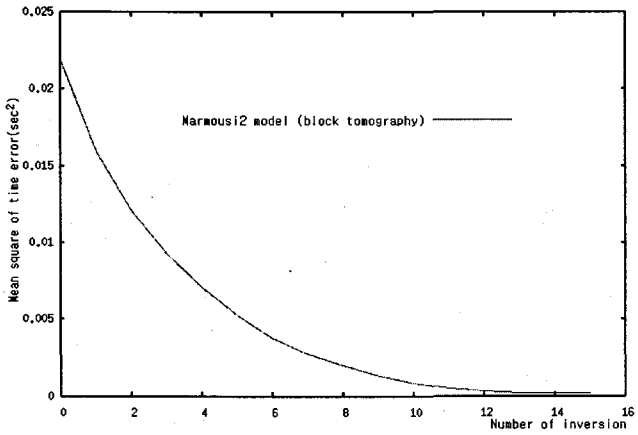

(b)

Fig. 5. The RMS error history of the traveltime inversion of the Marmousi-2 model by (a) the cell parameterization and (b) the block parameterization.

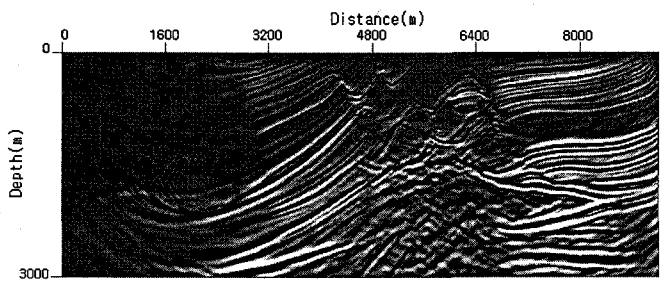

(a)

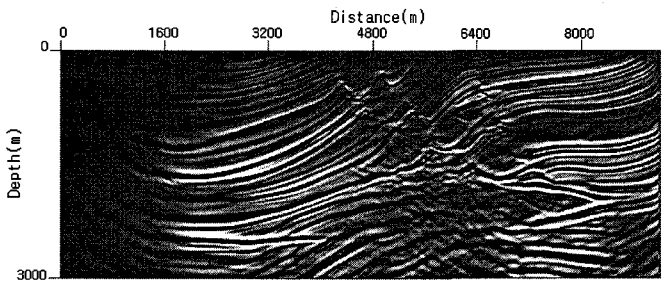

(b)

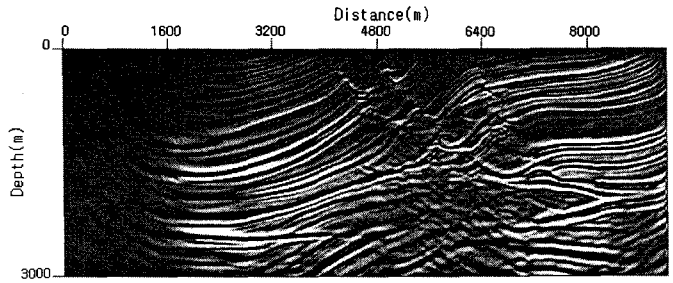

(c)

Fig. 6. Kirchhoff prestack depth migration image. (a) The prestack depth migration image where the initial velocity model is used for the migration, (b) the prestack depth migration image of the finally inverted velocity model via the cell parameterization, (c) the prestack depth migration image of the last inverted velocity model via the block parameterization.

4. Conclusions

In this paper, we developed a new algorithm to calculate the Frechêt derivative of the first arrival traveltime directly by using SWEET algorithm (Shin et al., 2002) and the finite element method.

In terms of computation costs, the block parameterization have been found to have an advantage over the cell parameterization without any deterioration to the quality of the initial velocity model for the prestack depth migration. Our numerical tests demonstrate that refraction tomography combined with a long offset survey can provide a smooth velocity model for the prestack depth migration.

We feel that the refraction tomography combined with the reflection tomography will be able to provide a smooth velocity model for the prestack depth migration. As to the calculation of the Frechêt derivative of the traveltime, we can extend our algorithm to the computation of Frechêt derivative of the amplitude of the first arrival event without any difficulty, thereby allowing us to incorporate the amplitude term to the refraction tomography. We plan to conduct future study on the inversion of minimizing the misfit of both the traveltime and the amplitude of the first arrival event.

References

Kreyszig, E., 1993, Advanced engineering mathmatics, 7th ed.: John Wiley and Sons, Inc.

Lines, L. R., and Treitel, S., 1984, A review of least-squares inversion and its application to geophysical problems: Geophys. Prosp. **32**, 159-186.

Martin, G. S., Marfurt, K. J., Larsen, S., 2002, Marmousi-2: an updated model for the investigation of AVO in structurally complex areas: **72**nd Ann. Internat. Mtg., Soc. Expl. Geophys., Expanded Abstracts, 1979-1982.

Pratt, R. G., 1999, Seismic waveform inversion in the frequency domain, Part 1: Theory and verification in a physical scale model: Geophysics, **64**, 888-901.

Shin, C. S., 1988, Nonlinear elastic wave inversion by blocky parameterization: Ph.D. thesis, Univ. of Tulsa.

Shin, C., Ha, J., Jeong, S., 1999, Refraction tomography by blocky parameterization: Journal of Seismic Exploration **8**, 143-156.

Shin, C., Yoon, K., Marfurt, K. J., Park, K., Yang, D., Lim, H., Chung, S., and Shin, S., 2001, Efficient calculation of a partial-derivative wavefield using reciprocity for seismic imaging and inversion: Geophysics, **66**, 1856-1863

Shin, C., Min, D., Marfurt, K. J., Lim, H., Yang, D., Cha, Y., Ko, S., Yoon, K., Ha, T., and Hong, S., 2002, Traveltime and amplitude calculations using the damped wave solution: Geophysics, **67**, 1637-1647.